Integrated Ferroelectrics, 2002, Vol. 50, pp. 21–32
Reprints available directly from the publisher
Photocopying permitted by license only

DOI: 10.1080/10584580290172053

Integration of Piezoelectric PZT Thin Films with Internal Electrodes into an Actuator Structure for MEMS Applications

M. HOFFMANN[1], T. LEUERER[2], R. LIEDTKE[1], U. BÖTTGER[1], W. MOKWA[2], R. WASER[1,3]

[1]Institute of Materials in Electrical Engineering II, University of Aachen, Sommerfeldstr 24, 52074 Aachen, Germany
[2] Institute of Materials in Electrical Engineering I, University of Aachen, Sommerfeldstr 24, 52074 Aachen, Germany
[3]Institute of Electroceramic Materials (EKM), Department IFF, Research Center Juelich, 52425 Juelich, Germany

(Received in final form October 15, 2002)

ABSTRACT

This paper presents the Finite-Element-Method (FEM) analyses, the processing, and the characterization of micro cantilever beams, which are driven by the transversal piezoelectric effect of two $PbZr_{0.45}Ti_{0.55}O_3$ (PZT) thin films with an internal platinum electrode. SiO_2/Si_3N_4 is used as elastic substrate for this stack. For the development of this thin film bimorph silicon bulk micro machining is used in combination with chemical solution deposition (CSD), sputter technology and reactive ion etching (RIE). For electrical and piezoelectric characterization of the PZT films CV-, hysteretic, and double beam laser interferometer measurements are carried out. The findings are compared to the FEM analyses and the results of a single piezoelectric layer design [1].

Keywords: micro actuator, $PbZr_{0.45}Ti_{0.55}O_3$, thin film bimorph, FE simulation

INTRODUCTION

The integration of piezoelectric thin films into micro cantilever actuators for electromechanical micro switch or relay applications provides interesting advantages in comparison to the electrostatic, electromagnetic, and electrothermic principles. These are high tip deflections at low applied voltages, low energy losses and a fast response behavior. Figure 1 shows (a) the scheme and (b) the microscopy picture of a realized piezoelectric cantilever actuator with an integrated PZT thin film for a micro relay application already presented in [2][3].

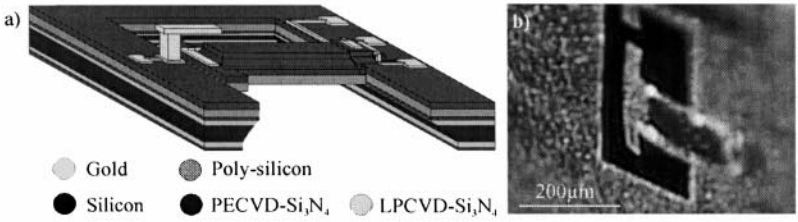

FIGURE 1: (a) Scheme of an integrated piezoelectric cantilever actuator for an electromechanical micro relay application. (b) Microscopy picture of the realized 190 µm long micro actuator, which was deflected by a driving voltage of 10 V.

The electromechanical characterization of this micro actuator reveal high tip displacements and resonance frequencies at low voltages but only small relay contact forces [1]. Hence, the development of a piezoelectric thin film multilayer stack for a micro cantilever actuator is very promisingly for an increase of the ratio of tip deflection, contact force respectively, and applied voltage [4][5]. Therefore, piezoelectric material and electrodes are deposited by turns. The different ceramic layers reinforce each other and this leads to an increase of the deflection, the force respectively, generated by this structure [6]. Due to different problems, e.g. contacting the internal electrodes, just research results for thin film stacks of multi layer capacitors (MLCs) are published [7][8].

Within this context the paper deals with the development of micro cantilever beams with two PZT films separated by an intermediate Pt electrode. In the following this design is termed "bimorph" in opposite to a "monomorph" with just one ceramic function film. First, the theory of an ideal bimorph without a support layer is discussed and compared to the FE simulation of a thin film bimorph and monomorph system with a substrate layer. Thereafter, a bimorph design, the processing and the integration steps are described. Finally, the micro cantilever structures and PZT films are characterized electrical and electromechanical.

THEORY AND FINITE-ELEMENT SIMULATION

The simplest electromechanical thin film micro actuator is a cantilever beam composed of an elastic polysilicon structural layer coated with a piezoelectric film, which forms the ideal monomorph structure. When an applied voltage drives the piezoelectric film to contract, the elastic layer resists this dimension change, leading to a bending deformation (figure 2 a)). If a second piezoelectric layer replaces the substrate, the ideal bimorph structure is obtained and two types of electrical connections can be used. One is the parallel connection,

where both layers posses the same polarization direction (figure 2 b)). The electric voltage is applied between the intermediate electrode and the top/bottom electrode. The second is the series connection, in which the two layers have an opposite polarization direction (figure 2 c)).

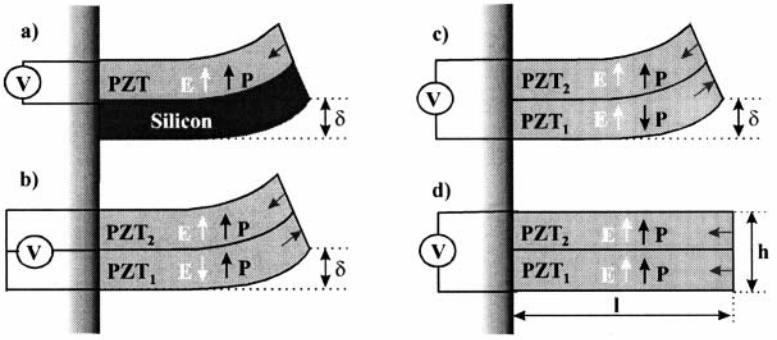

FIGURE 2: (a) Scheme of an ideal monomorph structure, (b) of an ideal bimorph structure in parallel, (c) in serial and (d) in a not working voltage connection.

The voltage is applied across the total thickness. In both cases, the below thin film expands while the upper layer contracts, but for the parallel case the driving voltage can be reduced to half the value used in the series case. In comparison to the monomorph the parallel ideal bimorph shows twice the displacement when the same voltage magnitude is applied [4]. The disadvantage of this structure is the limitation to voltages lower than the coercive voltage V_c. Otherwise the polarization of the below piezoelectric thin film switches and both films contract, leading to no deflection, like shown in figure 2 d).

For a real thin film bimorph a support layer is needed due to the fragility of the ceramic films. Hence, both films can contract for an upward deflection like in figure 3.

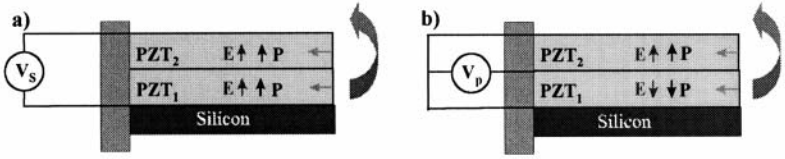

FIGURE 3: Scheme of a serial thin film bimorph (a) and of a parallel bimorph (b). Due to the needed Silicon support layer both piezoelectric films can contract for an upwards deflection δ and voltages higher than the coercive voltage V_c can be applied, because the electric field E is in parallel direction to the polarization P in both thin films.

The main advantage is that voltages higher than the coercive voltage can drive this bimorph system. In dependence of the ceramic polarization direction also two different types of electrical connections can be used. In the serial case both films have the same polarization direction (figure 3 a)) and in the parallel case they are polarized opposite (figure 3 b)). At the latter the driving voltage can be reduced again to the half in comparison to the serial connection.

For different analyses of the behavior of these last two cases finite-element simulations were carried out using the tool ANSYS 5.7. Due to the good match of measurement and FE simulation results of the above mentioned realized piezoelectric actuator for a micro relay [1], an additional PZT thin film and a Pt electrode extended the FE-model structure. For the calculation of the tip displacement δ and the resonance frequency f_R of the monomorph and bimorph micro actuators two dimensional plane elements with linear piezoelectric properties for small signal behavior were used.

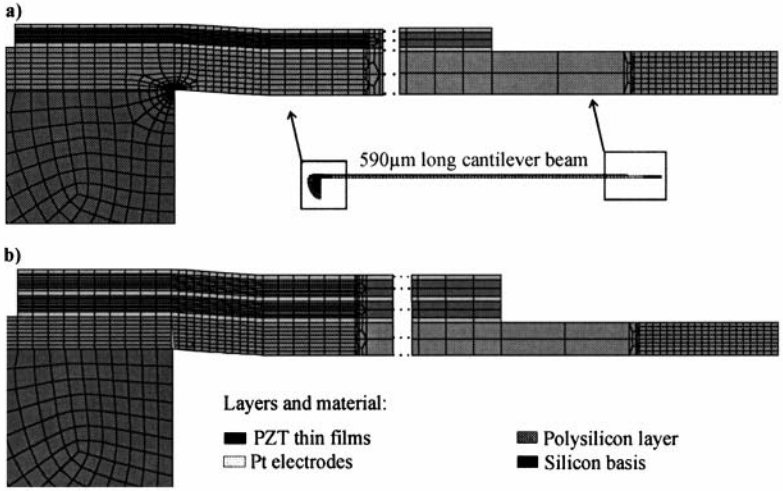

FIGURE 4: (a) Enlargement of a two dimensional 4-layer FE-model and the simulation grid of a 590 µm cantilever beam with one integrated piezoelectric PZT thin film. (b) Enlargement of a two dimensional 6-layer FE-model and the simulation grid of a 590 µm cantilever beam with two integrated piezoelectric PZT thin films and an internal electrode.

In figure 4 a) the FE-model of a 590 µm monomorph cantilever beam is shown. The important areas at the cantilever suspension and at the tip are enlarged. The grid of these parts is fine in comparison to the middle section of the actuator. The silicon bulk base, a 680 nm elastic poly-Si layer as substrate, a 100 nm Pt bottom and top electrode as well as one 350 nm PZT thin film were considered

in the model. The extended bimorph structure with the second PZT film, each of just 175 nm thickness, and a third 100 nm Pt electrode is shown in figure 4 b).

For the simulation the applied electrical field E was parallel to the polarization P in all PZT thin films, for the monomorph as well as for the bimorph. Therefore, each piezoelectric layer contracted. The simulated tip deflections δ of the monomorph and the bimorph as function of the cantilever length l for a driving voltage of $V = 10$ V can be analysed in figure 5 a). The bimorph structure with a length of 1000 µm reached a deflection of $\delta = 280$ µm. This is the threefold tip displacement of the monomorph with the same length.

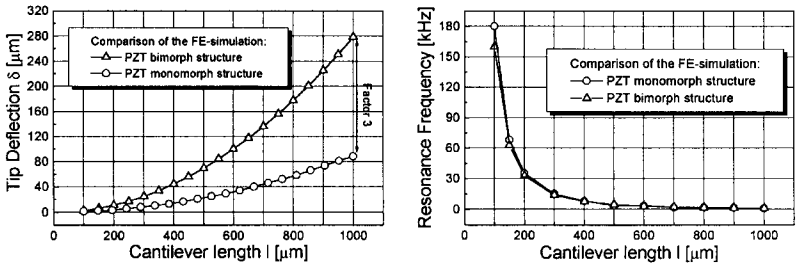

FIGURE 5: FE-analyses results of (a) the tip deflection δ at an applied driving voltage of 10 V and (b) the resonance frequency f_R of a PZT monomorph and bimorph structure in dependence of the cantilever length l.

The value is assumed to be to high in comparison to a real system, but also if the tip displacements of the bimorph just reach the same deflection the applied voltage can be reduced to half the value by a parallel connection of the films. The other possibility, where the below PZT film expands and the upper layer contracts, was simulated for $E < E_c$ as well. Here an increase of just 1.5 in opposite to the single layer structure was observed and might be explained by the substrate clamping. This case is not of importance for the aimed micro relay application, but interesting in comparison to the theory, predicting the double deflection for the bimorph. This result also indicates the functionality of the developed FE-model.

In figure 5 b) the resonance frequency f_R of both micro structures is shown as function of the actuator length l. The FE analysis of the bimorph actuator resulted in a slight decrease of the frequency in comparison to the monomorph. Two nearly compensating effects might explain this. Due to the third electrode the complete bimorph system becomes stiffer, resulting in an increase of the resonance. On the other hand the weight of the additional platinum electrode leads to a decrease. For the different lengths the both actuator structures have resonance frequencies between 0.5 kHz and 180 kHz.

The performed FE analyses indicated a high increase of the free cantilever deflection and just a slight decrease of the resonance frequency for the thin film bimorph. Therefore, the next chapter describes the design, the processing and first characterizations of such a micro actuator.

EXPERIMENTAL DETAILS

Bimorph-Design

Figure 6 shows the three-dimensional scheme of a micro electromechanical bimorph design. The cantilevers with lengths between l = 100-1000 µm and widths between w = 100-200 µm were integrated on oxidized 1'' silicon wafers.

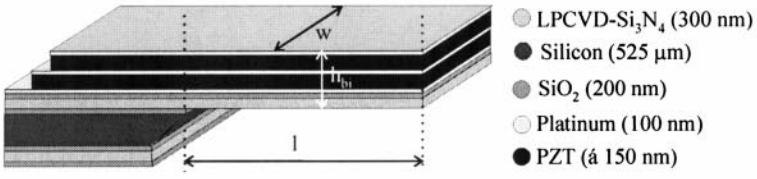

FIGURE 6: Three-dimensional scheme of the electromechanical micro actuator design with two integrated PZT thin films and an internal electrode.

First a LPCVD nitride and thermal oxide layer were deposited and structured on the wafer. They were used as mask on the backside for silicon bulk etching by TMAH and as etch stop layer on the top. The SiO_2/Si_3N_4 layers on the topside act as elastic cantilever substrate. The sputter deposition of a TiO_2/Pt bottom electrode is followed by a CSD step of the first PZT thin film. For the bimorph an internal Pt electrode is sputtered, then coated by another PZT thin film layer, and finally top contacted by Pt.

Processing and Integration

The sputtering processes were performed by using an Ardenne 500ES system. Reactive ion etching was executed on a Roth & Rau ECR-RIE Microsys 400 system and for the annealing steps an AST SHS100MA rapid thermal annealing (RTA) system was used. The oxidation of the (100)-oriented 1'' silicon wafer and the LPCVD-Si_3N_4 process were carried out by the ISI at the Research Center Juelich (figure 7 step 1).

Figure 7 shows the complete scheme of all proceeding steps. The SiO_2/Si_3N_4 backside layer was reactive ion etched (step 2). An etching rate of 44 nm/min was reached by a CF_4/CHF_3/Ar-plasma (5:5:1) at an applied bias of 250 V, a chamber pressure of 4 µbar and a substrate temperature of –15 °C. Thereafter, the (111)-oriented TiO_2/Pt bottom electrode was argon sputtered and annealed in

O_2 atmosphere by a RTA step at 700 °C for 5 min (step 3). The production of the PZT stock solution and the CSD process are described detailed in [2][3]. For the bimorph a 150 nm ceramic thin film was deposited first (step 4) and contacted by an argon sputtered intermediate Pt electrode (step 5). The CSD process was carried out once again for the upper 150 nm PZT thin film. This film was top contacted also by a Pt electrode (step 6).

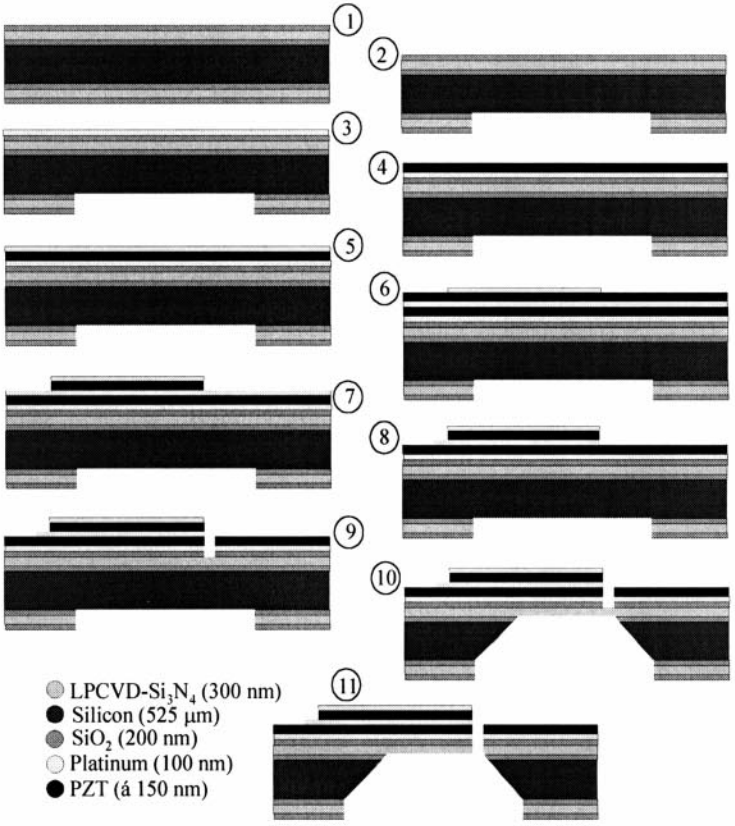

FIGURE 7: Two-dimensional scheme of the fabrication process of the electromechanical micro actuator with two integrated PZT thin films and an internal electrode.

Identical deposition conditions where used for the Pt top electrodes and the intermediate electrode. The Pt electrodes were always etched by an Ar/O_2-plasma (5:1) at an applied bias of 300 V, a chamber pressure of 8 µbar and a substrate temperature of –15 °C (steps 6 and 8). This process yielded an etching rate of 13 nm/min. The PZT films were structured by an ECR-RIE process

(steps 7 and 9). To protect the resist, the first 100 nm were etched with the parameters used for the bottom electrode as well. Such conditions enabled a ceramic etching rate of 11 nm/min. The last 50 nm of each ceramic film were etched by a CF_4/Ar-plasma (5:1) at an applied bias of 250 V, a chamber pressure of 4 µbar and a substrate temperature of –15 °C. This process supplied an etching rate of 11 nm/min, whereas, Pt was etched at 2 nm/min (in comparison to 13 nm/min using the electrode parameters). Thus it was possible to structure the piezoelectric ceramic very selective and homogeneous without fences by slightly over-etching of the films. The SiO_2/Si_3N_4 front side layer was reactive ion etched by the same process used for the backside (step 10). In the future the Si-bulk will be wet chemically removed by a TMAH (20 %) process providing an etching rate of 32 µm/h at 85 °C (step 11). This last step for the processed 1'' wafers is still under development.

The optical characterization methods document the precision of the deposition and integration processes as described above.

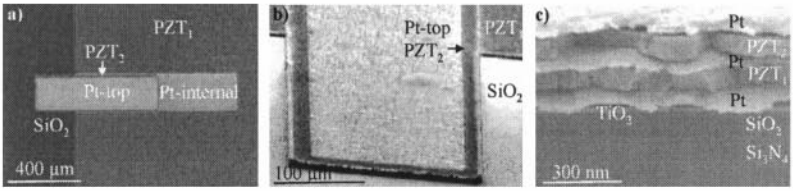

FIGURE 8: (a) Microscopy picture of an integrated bimorph cantilever, (b) SEM picture of the structured 200 µm cantilever in the silicon oxide window, and (c) SEM micrograph of the cross section of the structure.

In figure 8 a) a microscopy picture of an integrated bimorph actuator is given. For microstructure and fabrication control scanning electron microscopy (SEM) was carried out. The SEM picture of a 200 µm bimorph structure is shown in figure 8 b). Whereas the cross section of an integrated bimorph structure with the three Pt electrodes and the two PZT thin film layers deposited on SiO_2/Si_3N_4 can be seen in figure 8 c).

Electrical and Electromechanical Characterization

Both integrated ceramic PZT thin films of the bimorph structure were electrical characterized by polarization and CV-measurements. For the hysteretic measurements the FE-module of an aixACCT TF Analyzer was used. Whereas CV-loops were recorded by using a 50 mV rms AC voltage and a slow bias voltage sweep of 50 mV/s by means of a LCR meter HP4284A. Figure 9 a) shows the hysteretic loop of the upper 150 nm PZT film at room temperature. The remnant polarization was determined to P_r = 17 µC/cm^2 and the coercive

voltage to V_c = 0.56 V (E_c = 37 kV/cm). The measurement of the relative permittivity at room temperature is shown in figure 9 b).

At a voltage of V = 0 V a relative permittivity of ε_r = 993 was measured. The below PZT thin film indicated nearly the same electrical behavior. The values are slightly smaller than the ones reported for the cantilever structure with a single PZT layer with a thickness of 350 nm [2]. This might be explained by a thickness dependence and interface capacities between the ceramic film and the electrodes, which become more relevant for decreasing film thickness [9].

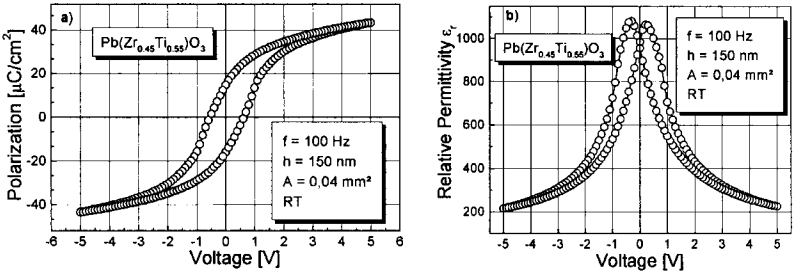

FIGURE 9: (a) Hysteretic- and (b) CV-measurement of the integrated upper PZT thin film of the structured bimorph cantilever. Nearly the same values were measured for the PZT thin film below.

Based on the results of the hysteretic and CV-measurements a roughly estimation of the piezoelectric coefficient d_{31}, which is a measure for the tip deflection of the cantilever structures, can approximately be derived by [10][11]:

$$d_{31} = 2\varepsilon_0 \varepsilon_r P_r Q_{12} \cong -0.43 d_{33} \qquad (1)$$

whereby the electrostrictive coefficients Q_{12pzt} = -3.1*10^{-2} m4/C^2 for the PZT bulk ceramic is assumed as nearly constant [11]. The last equation term for single crystals often is also used for thin film estimations [10][11]. Therefore, the piezoelectric coefficients can be calculated to d_{31} = -92 pC/N and d_{33} = 215 pC/N. These first values are to high, because the clamping effect of the substrate layer and the electrodes are not taken into account by the used bulk equations.

Due to this roughly estimation of the piezoelectric properties the converse d_{33} coefficient was also measured directly by using a double beam laser interferometer. For this purpose a thin film capacitor structure consisting of a 100 nm TiO_2/Pt bottom electrode, a 300 nm CSD thin film of the integrated PZT material and a 100 nm Pt top electrode with a pad size of 1 mm² was produced on a double side polished Si wafer. The backside of the wafer was covered with gold by vapor deposition for a better laser beam reflection. For the measurement

all optical components were placed inside a thermo-shielded chamber to avoid any drift or vibration of these components. All electrical equipment, e.g. lock-in amplifier, function generator, oscilloscope, and the laser controller are PC controlled and placed outside the chamber. The advantage of a double beam laser interferometer in opposite to a single beam laser interferometer is the measurement on the top- and the backside of the wafer in one run. Hence, bending effects are subtracted immediately. Therefore, the laser beam with a wavelength of 632.8 nm is split into a reference beam and a measurement beam. The measurement beam is directed first to the backside of the capacitor structure and then to the 1 mm^2 top contact by mirrors, $\lambda/4$ plates, and polarized beam splitters. Finally, it is superposed with the reference beam and the intensity is measured with a photo detector. With this setup a resolution in the range of 10^{-2} Å is obtained [12]. For measuring the d_{33} coefficient an oscillation level of 200 mV at a frequency of 2 kHz is applied at different DC bias voltages. Through the longitudinal piezoelectric effect, the PZT film thickness changes and causes a change of the intensity of the superimposed beam. Since the light intensity is proportional to the piezoelectric coefficient it is possible to calculate the converse d_{33} coefficient, which is a better indication for the expected d_{31} coefficient by equation (1). Figure 10 shows the measured piezoelectric coefficient d_{33} as function of the applied voltage at room temperature and a frequency of 2 kHz. The remnant value at a voltage $V = 0$ V is determined to d_{33} = 98 pC/N, equivalent to $d_{31} = -41$ pC/N. These values are more reasonable in comparison to the first estimations and also in good accordance to literature data [13][14]. Taking into account the measured relative permittivity of $\varepsilon_r = 993$ the coupling coefficient k_{31} can be calculated by [4]:

$$k_{31} = d_{31}\left(\varepsilon_r s_{11}\right)^{-0.5} \qquad (2)$$

to $k_{31pzt} = 0.26 \sim 26$ %, wherein the compliance for PZT is $s_{11pzt} = 14.29$ $\mu m^2/N$ [15].

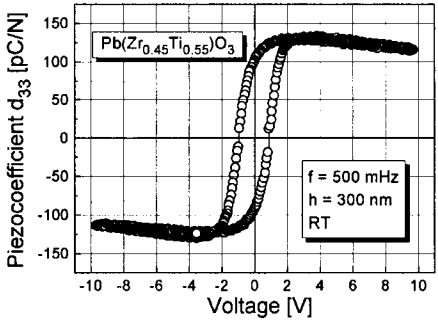

FIGURE 10: Laser interferometer measurement of the piezoelectric coefficient d_{33} as function of the applied voltage at a 300 nm PZT thin film capacitor.

This value is in the range of PZT bulk ceramics [15] and has to be verified by first measurements at free bending bimorph structures in the future. The characterization results of the bimorph structures are very promising for an effective micro actuator realization.

SUMMARY

This work presented the results of the development of a $Pb(Zr_{0.45}Ti_{0.55})O_3$ thin film bimorph. First the executed 2D-FE analysis results of the free tip deflection δ and the resonance frequency f_R of a monomorph were compared to a bimorph structure. Due to the substrate of the bimorph both $PZT_{45/55}$ layers are allowed to contract. Therefore, voltages higher than the coercive voltage can be applied to the ceramic films without switching the polarization. This leads to a threefold higher deflection for a serial connection of the bimorph compared to the values of the monomorph cantilevers at the same driving voltage. For a parallel connection and opposite polarization direction the applied voltage can also be reduced to half the value of the serial case. For bimorph cantilever lengths of l = 100-1000 µm the FE simulation results showed tip deflections of δ = 10-280 µm and resonance frequencies of f_R = 0.5-180 kHz. The frequencies are slightly smaller than the monomorph ones.

In the second part, the design of a bimorph structure with 150 nm $PZT_{45/55}$ CSD thin films was realized. The processing by sputtering, CSD, reactive ion etching, and bulk silicon etching with TMAH was described in detail and documented by microscopy and SEM. Electrical and piezoelectric characterizations approved the functionality of the successful integrated stack structures. For both $PZT_{45/55}$ films of the bimorph the remnant polarization was determined to P_r = 17 µC/cm^2, the coercive voltage to E_c = 37 kV/cm, and the relative permittivity to ε_r = 993. The piezoelectric coefficient d_{33} = 98 pC/N of the PZT ceramic was measured by a double beam laser interferometer. The determination of d_{31} = -41 pC/N provided a coupling coefficient of k_{31} = 26 %.

These simulation and first characterization results of the realized thin film stacks indicate an effective actuator behavior for free standing bimorph cantilevers. This has to be confirmed by laser vibration measurements of the tip displacement after completion of bulk silicon etching from the wafer backside by TMAH.

REFERENCES

[1] Hoffmann M, Leuerer T, Krüger C, Böttger U, Mokwa W, and Waser R: Mat. Res. Soc. Symp. Proc., Vol. 688, C 5.9.1-8 (2002).

[2] Hoffmann M, Küppers H, Schneller T, Böttger U, Schnakenberg U, Mokwa W, Waser R: Int. Sym. Appl. Ferro. Proc., Vol. 1, pp. 519-524 (2000).

[3] Küppers H, Hoffmann M, Leuerer T, Schneller T, Böttger U, Waser R, Mokwa W, and Schnakenberg U: Transducers'01, Vol. 2, pp. 1018-1021 (2001).

[4] Polla DL and Robbins WP: Academic Press, London, by Taylor DJ, pp. 203-226 (2000).

[5] H. Schaumburg: B. G. Teubener, Stuttgart, Germany (1994).

[6] Smits JG, Choi WS: IEEE Trans. Ultra., Ferro., Freq. Control, Vol. 38, pp. 256-270 (1991).

[7] Tagantsev AK, Kholkin AL, Brooks EL, Setter N: Int. Ferro., Vol. 10, pp. 189-204 (1997).

[8] Grossmann M, Slowak R, Hoffmann W, John H, Waser R: Proc. ECC VI, Montreux (1998).

[9] Lee SH, Joo HJ, Kim PJ, Jung JH, Ryu MK Lee SS, and Jang MS: J. Kor. Phys. Soc., Vol. 35, pp. 1172-1175 (1999).

[10] Maiwa H, Maria J, Christman J, Kim S, Streiffer S, Kingon A: Int. Ferro., Vol. 24, pp.139-146 (1999).

[11] Abe T, Reed ML: IEEE MEMS, pp. 164-169 (1994).

[12] Gerber P: Diploma Thesis, IWE, RWTH Aachen, Germany (2001).

[13] Muralt P: Int. Ferro., Vol. 17, pp. 297-307 (1997).

[14] Dubois MA, Muralt P, Taylor DV, Hiboux S: Int. Ferro., Vol. 22, pp. 535-543 (1998).

[15] Xu Y: North-Holland, Amsterdam (1991).